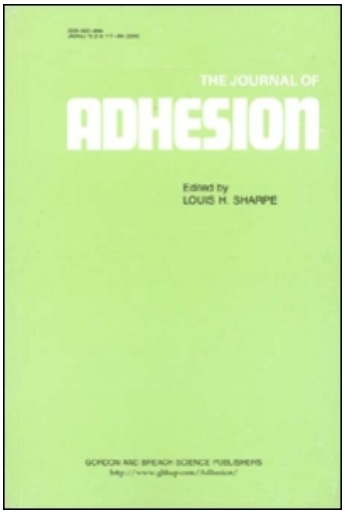

The Journal of Adhesion

Publication details, including instructions for authors and subscription information:
http://www.informaworld.com/smpp/title~content=t713453635

Constant Displacement Rate Method for Testing Epoxy Adhesive Bonds

D. R. Arnott[a]; M. R. Kindermann[a]
[a] Airframes and Engines Division, Aeronautical and Maritime Research Laboratory, Defence Science and Technology Organisation, Victoria, Australia

To cite this Article Arnott, D. R. and Kindermann, M. R.(1995) 'Constant Displacement Rate Method for Testing Epoxy Adhesive Bonds', The Journal of Adhesion, 48: 1, 85 — 100
To link to this Article: DOI: 10.1080/00218469508028156
URL: http://dx.doi.org/10.1080/00218469508028156

J. Adhesion, 1995, Vol. 48, pp. 85–100
Reprints available directly from the publisher
Photocopying permitted by license only

Constant Displacement Rate Method for Testing Epoxy Adhesive Bonds

D. R. ARNOTT and M. R. KINDERMANN

Defence Science and Technology Organisation, Airframes and Engines Division, Aeronautical and Maritime Research Laboratory, 506 Lorimer St., Fishermen's Bend, Melbourne, Victoria, 3207, Australia

(Received November 18, 1993; in final form May 24, 1994)

A constant load-point displacement rate method is used to test double-cantilever-beam specimens of 2024–T3 aluminium alloy bonded with AF126 adhesive. The elastic energy release rate, G_1, was calculated from measured values of load and load-point displacement. Measurements in humid air at 50°C showed that G_1 depended strongly on load-point displacement rate. At high rates, the bond was not degraded and G_1 was equivalent to G_{1c}. At very low rates, the bond was degraded and G_1 was equivalent to G_{1scc}. In a region between these extremes, G_1 was sensitive to load-point displacement rate because moisture degraded the bond at a rate similar to the crack velocity. Selection of data where G_1 was unstable with load-point displacement rate leads to a crack velocity, which may be used as a bond durability indicator.

KEY WORDS Adhesive bond; epoxy film adhesive; aluminium alloy; accelerated durability testing.

1 INTRODUCTION

The durability of structural adhesive bonds between metal components is currently estimated with the Boeing wedge test.[1] There are difficulties in applying quantitative fracture mechanics to this test. This paper describes a new constant displacement-rate test (CDRT)[2] which addresses these difficulties.

1.1 Boeing Wedge Test

The Boeing wedge test (Figure 1a) is widely used for comparing adhesive bond durabilities under warm and wet conditions, (50°C and 98% humidity).[1,3] One end of a double-cantilever beam (DCB) specimen is opened to a specified and constant crack opening displacement using a wedge. This test is particularly suited to ranking qualitatively the efficacies of adherend surface treatments.

Several authors[4–7] have applied linear elastic fracture mechanics to this problem. Here, the elastic energy stored in the adherends gives rise to a force extending the crack. These authors have assumed that no plastic deformation of the adherends occurs during testing. The elastic energy release rate (or crack extension force), G_1, is

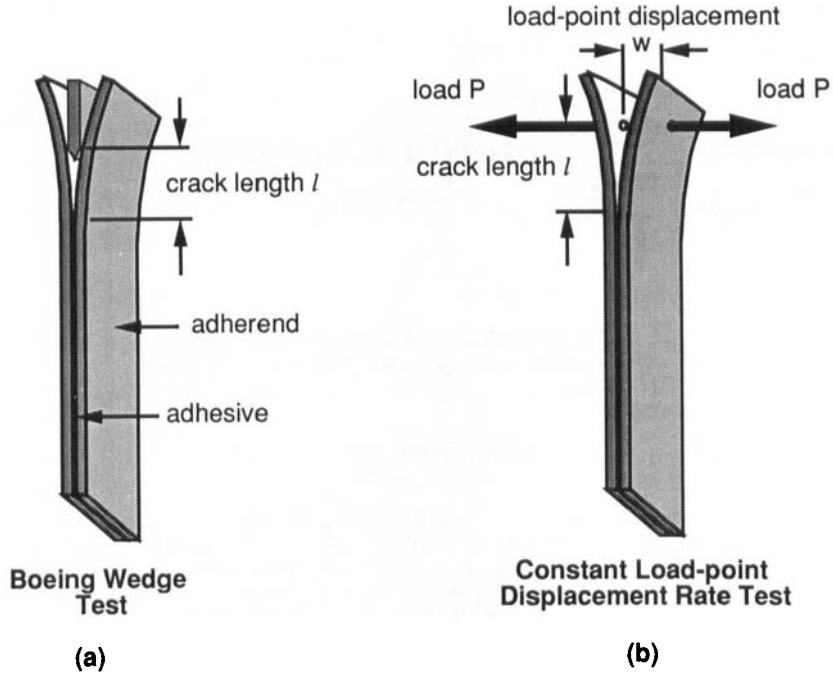

FIGURE 1 Bonded double-cantilever beam specimen.

estimated[5-8] using the equation:

$$G_1 = \left[\frac{3h^3Ew^2}{16l^4}\right] \tag{1}$$

where h is the adherend thickness, E its Young's modulus, l its effective length and w is the load-point displacement. Equation (1) assumes that the crack length is much greater than the adherend thickness. By neglecting compensation for shear or bending, the error in determining G_1 is less than 3 per cent for typical crack lengths and adherend thicknesses.[9] Some authors correct the crack length for adherend rotation.[9,10] This correction has a pronounced effect on G_1.

Equation (1) shows that G_1 decreases as l increases. Crack growth effectively ceases when the elastic energy release rate falls just below a critical value, G_{1c}, equal to the fracture energy of the bond. In dry air, Cognard[6] states that crack growth essentially ceases within 24 hours of wedge insertion. In humid air, the fracture toughness of material ahead of the crack tip may also change with time. Hardwick *et al.*[5] defined an arbitrary threshold value of G_1, evaluated after a long exposure, greater than 200 hours, which he called G_{1scc}. Baker[4] evaluated G_1 initially and after 48 hours, from which he defined a normalised G_θ. Here, testing time was minimised and G_θ gave an indication of bond durability.

G_1 clearly depends on estimates of l in the Boeing wedge test. The crack length cannot be measured accurately due to the uncertainty in locating the crack tip. Thus, the precision of G_1 is poor since l is usually equated to crack length[5,6,9]. Hence, there is clear motivation to develop a test that eliminates the need to measure l.

1.2 Constant Dusokacenebt Rate Test (CDRT)

A bonded DCB specimen is opened at a constant load-point displacement rate (Figure 1b). The rate selected strongly influences the crack velocity. In humid air, the load-point displacement rate, dw/dt, can be selected to drive the crack at a velocity that is either faster or slower than the rate of degradation of the bond ahead of the crack tip.

The application of fracture mechanics to the CDRT leads to expressions for both the elastic energy release rate and crack velocity.

1.2.1 Elastic Energy Release Rate

The elastic energy release rate can be written implicitly in terms of the load, P, and load-point displacement, w, as:

$$w = \left[\frac{Eh^3 G_1^3 b^4}{27}\right]^{1/2} \frac{1}{P^2} \tag{2}$$

where b is the width of the adherends. Equation (2) is derived using thin-beam approximations[6-10] and assumes negligible plastic deformation in the adherends. Where w varies linearly with P^{-2}, G_1 becomes a constant of the test.

1.2.2 Crack Velocity

The "crack length" is taken as the linear distance from the centre of loading to the crack tip. The effective length, l, of the cantilevers is greater than the crack length by a constant difference.[9,10] Thus, the rate of increase in l (dl/dt) is equal to the crack velocity. For the case where G_1 is time invariant, differentiation of equation (1) gives the crack velocity, dl/dt, as:

$$\frac{dl}{dt} = \frac{1}{8l}\left[\frac{3Eh^3}{G_1}\right]^{1/2} \frac{dw}{dt} \tag{3}$$

For the case where G_1 and dw/dt are both constant, the crack velocity will decrease as the crack advances. Thus, for a crack advancing from 40 to 120 mm under these conditions, the crack velocity at 120 mm is one third of that at 40 mm. However, the magnitude of this change in crack velocity is small compared with the three-decade range of dw/dt selected.

From equations (2) and (3), an alternative statement of the crack velocity is:

$$\frac{dl}{dt} = \frac{3}{4b}\left(\frac{P}{G_1}\right)\frac{dw}{dt} \tag{4}$$

1.2.3 Stability

Gurney *et al.*[8,11] have analysed quasi-static crack propagation under monotonically increasing displacement. This analysis suggests that crack propagation is stable provided that the elastic energy release rate does not decrease rapidly with increasing crack length.

1.2.4 Plastic Deformation of the Adherends

Gurney and Amling[8] establish that the onset of plastic deformation occurs at a critical beam thickness given by:

$$h_{crit} = \frac{3G_1 E}{\sigma_y^2} \tag{5}$$

where σ_y is the yield stress of the material. The constant rate of opening of the DCB specimen in the CDRT contrasts with the impulsive load applied to the adherends in the Boeing wedge test. The slow opening of the DCB specimen in the CDRT will produce a lower initial value of G_1 than the Boeing wedge test and will thus tend to minimise any plastic bending of the adherends.

2 EXPERIMENTAL

Plates of clad 2024–T3 aluminium alloy (152.4 × 152.4 × 3.2 mm) were machined to receive hemispherical-headed loading screws (Figure 2). These plates, degreased with AR grade methylethylketone, were abraded with a dry Nylon scouring pad (Scotch-

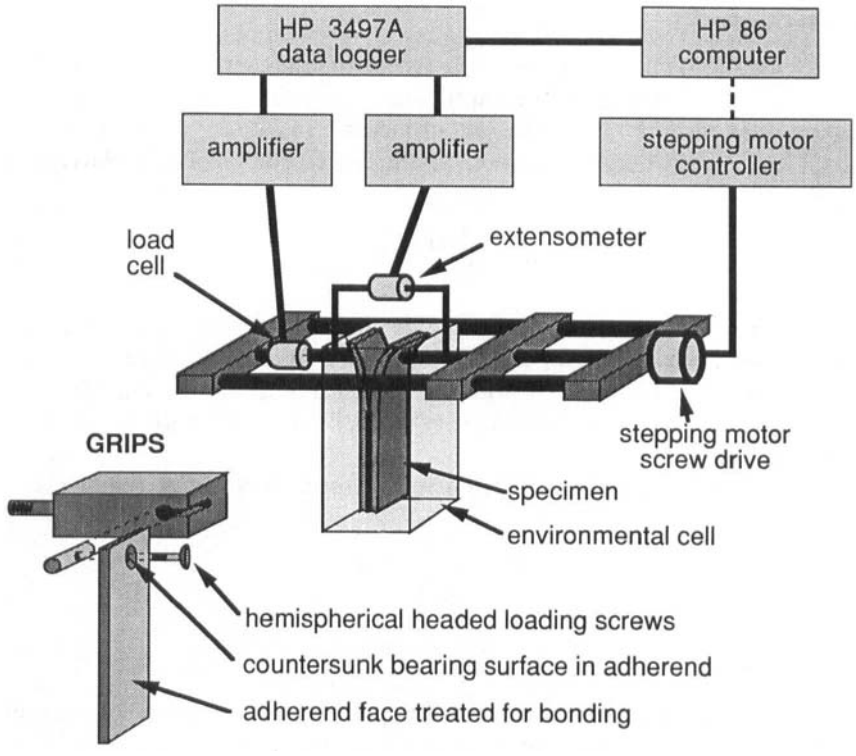

FIGURE 2 A diagram of the constant displacement-rate test showing the specimen configuration, loading grips and environmental cell.

Brite[R] [a]) and blown clean with pressurised dry nitrogen. Next, the plates were grit-blasted with 50 micron alumina carried in a stream of dry, oil-free nitrogen at a pressure of 550 kPa. Subsequently, the plates were cleaned with pressurised dry nitrogen. Paired plates with loading screws installed were bonded with AF126 film adhesive[a]. The adhesive was cured in a press with the surfaces loaded to 96 kPa. The temperature was raised to 120°C over 35 minutes and was held for 1.5 hours. Five DCB specimens were cut from the bonded plates, machined without lubricant to a final width of 25.4 mm and stored over a silica-gel desiccant.

The specimens were heated to 50°C in a water-jacketted environmental cell as shown in Figure 2 and tested at values of dw/dt ranging from 50 mm/hr to 5 μm/hr. Some tests were conducted in dry air and the remainder in condensing humidity. A foil cover was placed over the upper end of the specimen to prevent condensed water entering the crack. The DCB specimen was opened at a constant rate in a loading frame as shown in Figure 2. The cross-head screw was driven by a stepping motor, pulsed at a selectable rate from a crystal-controlled clock. The load, P, and load-point displacement, w, were recorded at fixed intervals. The crack length was monitored with a travelling microscope. Two methods for calculating crack velocity were used. In the "direct" method, crack velocities were calculated using crack lengths measured as a function of time. In the "compliance" method, equation (4) was used.

Irreversible plastic deformation in the adherends was estimated from the residual load-point displacement of a single cantilevered beam 25.4 mm wide by 3.2 mm thick. Beam lengths from 10 to 140 mm were tested with similar loads to those used in the CDRT. Residual plastic bending was less than 4 per cent of the deflection at maximum load and considered negligible. The validity of elastic energy release rate calculations depends on adherend thickness as described by equation (5). For 2024–T3 aluminium alloy sheet of 3.2 mm thickness and $\sigma_y = 3.61 \times 10^8$ Pa, the threshold of G_1 for plastic deformation in the adherends is 1900 Jm^{-2}.

3 RESULTS

A typical plot of load *versus* time (or load-point displacement) for a bonded DCB specimen opened at constant dw/dt is shown in Figure 3. Elastic energy stored in the adherends during the phase of rising load initiates the crack, after which the load decreases with increasing w. Attention was focussed on observations recorded after reaching maximum load. In principle, the zero of load-point displacement should be taken at crack initiation. This condition cannot be measured to a high degree of precision and calculations which rely on absolute values of w were avoided.

The functional relation between w and P^{-2} described in equation (2) was investigated graphically. Figure 4 shows that plots of log (P) *versus* log (w) have gradients of $-(0.5 \pm 0.05)$. The offset in these graphs indicate that G_1 is sensitive to humidity. Figure 5 shows an alternative plot of w *versus* P^{-2}. G_1 is calculated from the gradient of a least-squares linear fit where the constants for the 2024–T3 adherends are:

$$E = 7.3 \times 10^{10} \text{ Pa}, h = 3.2 \times 10^{-3} \text{ m}, b = 2.54 \times 10^{-2} \text{ m and } \sigma_y = 3.61 \times 10^8 \text{ Pa}.$$

[a] Minnesota Mining and Manufacturing Company (3M Co.).

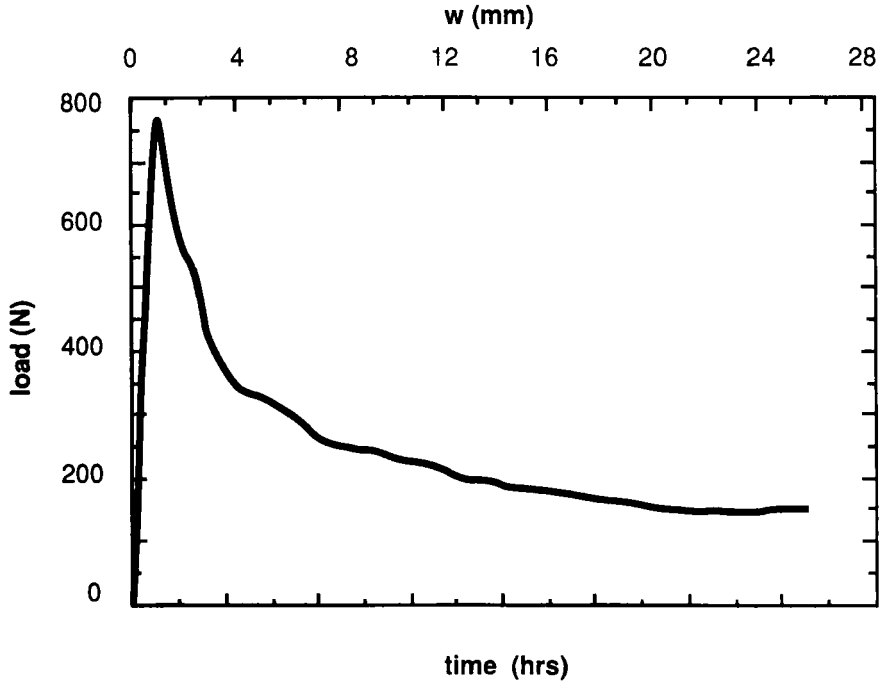

FIGURE 3 A representative plot of P *versus* time (and w) during separation of a bonded DCB specimen in dry air at $dw/dt = 3.5$ mm/hr.

The elastic energy release rate, G_1, is $1530\,\mathrm{Jm}^{-2}$ for the example shown in Figure 5. This value is lower than that shown by Figure 4 and is due to the scatter in G_1 measurements between specimens. All subsequent G_1 values were calculated using this linear least-squares routine. The intercept w' shown in Figure 5 is the effective value of w at an apparent "infinite load" condition and is believed to represent crack initiation. For some tests conducted in humid air, more than one linear region in the w *versus* P^{-2} plots have been observed. These linear segments are distinct and G_1 is calculated for each segment.

Zero load-point displacement was chosen when the load just commenced to rise (Figure 3). Figure 6 shows instantaneous G_1 as a function of a corrected load-point displacement, w_c ($= w - w^*$), where w^* is an arbitrary initial adjusting value. Figure 6 also shows that for $w^* = 0.0$ and 0.4 mm, G_1 overshoots the mean whereas for $w^* = 1.0$ mm, G_1 undershoots the mean. The $w^* = 0.7$ mm ($= w'$) is shown as a bold plot (Figure 6 (iv)). Conditions in Figure 6 are the same as those in Figure 5, where G_1 was shown to be well behaved for load-point displacements greater than 0.7 mm.

Figure 7 shows the inverse relation between the crack velocity and measured crack length. This inverse relation is typical of CDRT experiments where G_1 is constant. In Figure 7, the crack velocity was determined using direct optical measurement. The linear fit is consistent with equation (3) where $dw/dt = 35$ mm/hr and $G_1 = 1750\,\mathrm{Jm}^{-2}$.

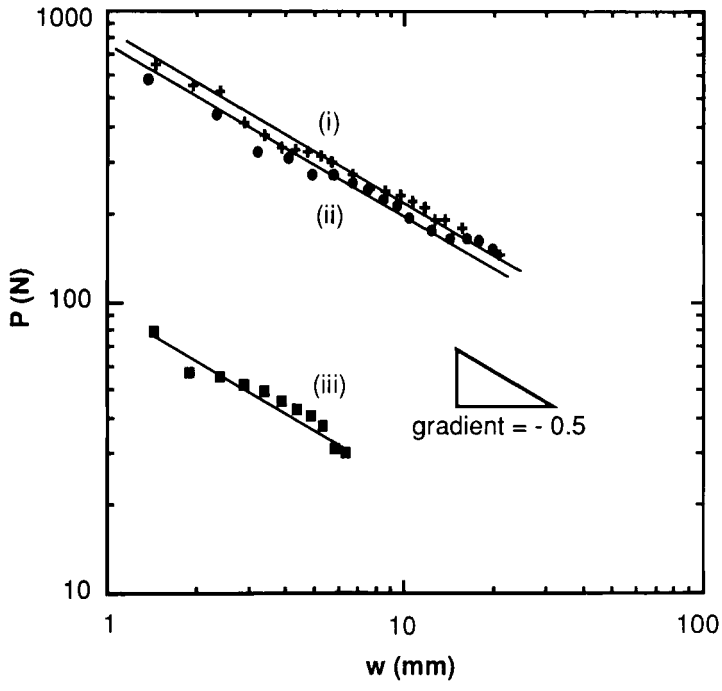

FIGURE 4 Plots of P *versus* w on a logarithmic scale for three test conditions: (i) warm dry air and $dw/dt = 3.5$ mm/hr (crosses). ($G_1 \approx 1750\,\mathrm{Jm}^{-2}$). (ii) warm humid air and $dw/dt = 0.35$ mm/hr (circles). ($G_1 \approx 1700\,\mathrm{Jm}^{-2}$). (iii) warm humid air and $dw/dt = 0.035$ mm/hr (squares). ($G_1 \approx 110\,\mathrm{Jm}^{-2}$). The lines of best fit were calculated using equation (2) with G_1 as the only parameter changing with test conditions.

A plot of G_1 *versus* dw/dt for specimens with grit-blasted adherend surfaces is shown in Figure 8. Dry air tests gave an almost constant G_1 with dw/dt (Figure 8 curve (i)) whereas humid air tests gave a large reduction in G_1 when dw/dt was less than 7 mm/hr (Figure 8 curve (ii)). As dw/dt was decreased to very low values (less than 0.5 mm/hr), G_1 approached a lower plateau. Figure 8 curve (ii) also shows a range in dw/dt (0.2 to 4 mm/hr) where G_1 was unstable. G_1 was stable at both higher and lower values of dw/dt.

In some humid air tests conducted in the unstable range of dw/dt, the w *versus* P^{-2} plot produced two linear segments. In these tests, a comparatively abrupt change occurred between the linear segments. Here, the linear segment evaluated early in the test showed that G_1 tended toward the upper plateau, whereas the one evaluated later tended toward the lower plateau.

Fracture surfaces of specimens tested in dry air show that failure had occurred principally in the adhesive film (Figure 9(a)). The fracture surface of a specimen tested in humid air at 36 mm/hr revealed large areas of "adhesive" failure (where failure had occurred at the interface) and evidence of corrosion (Figure 9(b)). The specimen tested in humid air at 3.6 mm/hr showed "adhesive" failure had occurred principally along one adherend surface (Figure 9(c)).

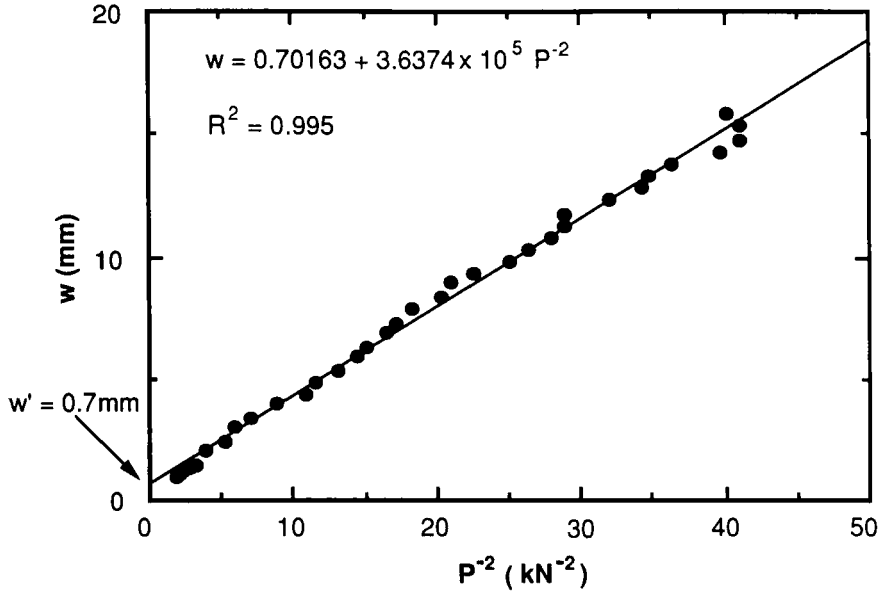

FIGURE 5 A plot of w *versus* P^{-2} with at least-squares linear fit. Test conducted in warm dry air at $dw/dt = 0.35$ mm/hr.

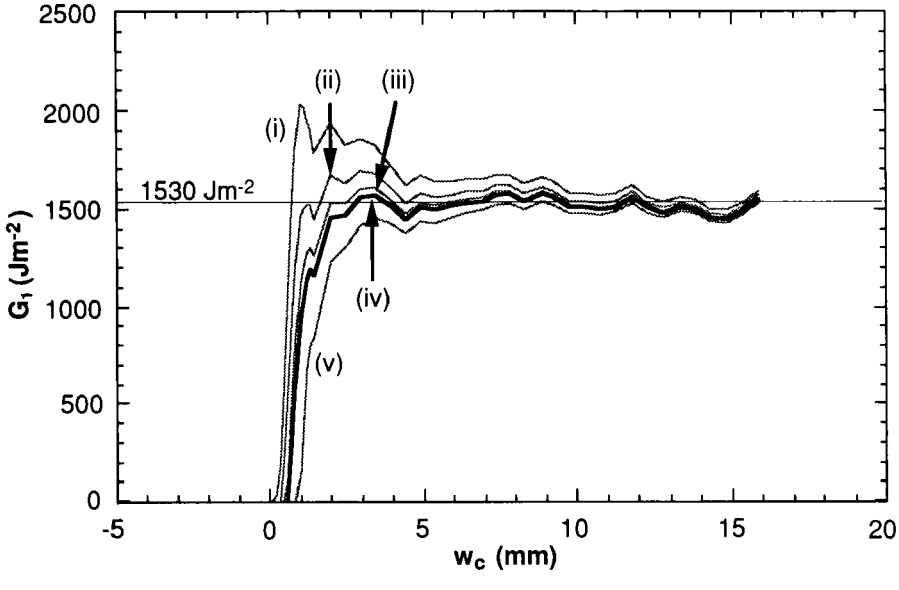

FIGURE 6 Plots of instantaneous G_1 *versus* w_c for five arbitrary initial value w^*. G_1 was calculated from equation (2) with instantaneous values of P and w_c ($= w - w^*$). The test was conducted in warm dry air at $dw/dt = 0.35$ mm/hr. (i) $w^* = 0.0$ mm. (ii) $w^* = 0.4$ mm. (iii) $w^* = 0.6$ mm. (iv) $w^* = 0.7$ mm. (v) $w^* = 1.0$ mm.

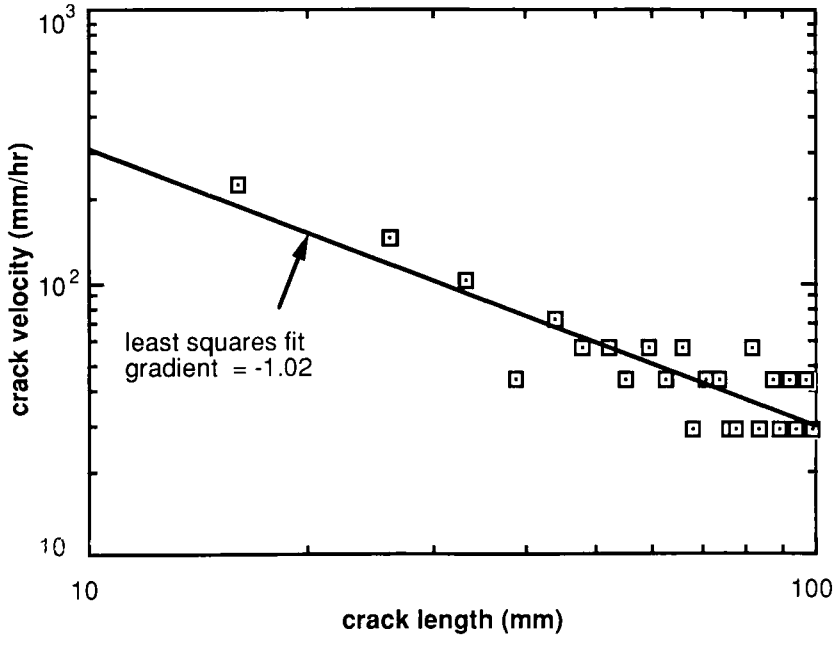

FIGURE 7 Plot of measured crack velocity *versus* measured crack length on a logarithmic scale for tests conducted in warm dry air at $dw/dt = 35$ mm/hr. The solid line is a least-squares linear fit to the data.

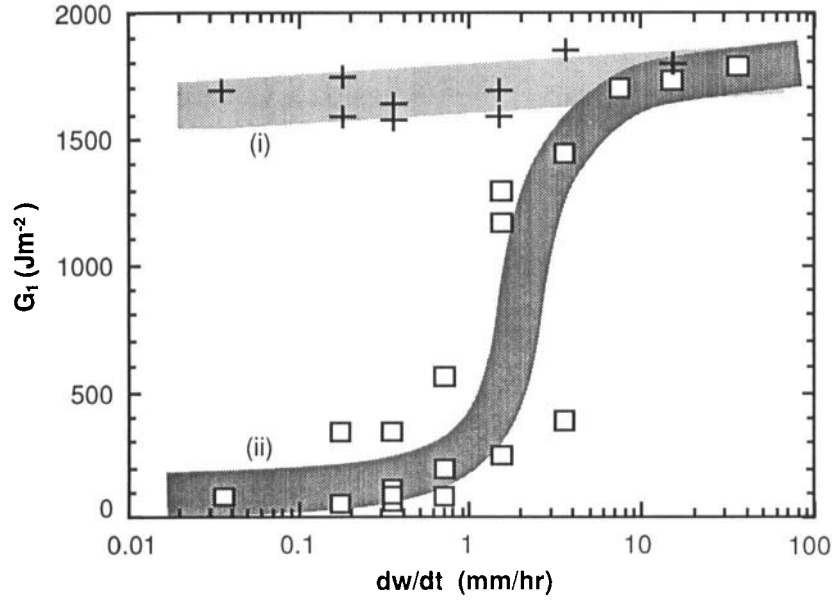

FIGURE 8 Plots of G_1 *versus* dw/dt for two specimens with grit-blasted adherends.(i) warm dry air. (ii) warm humid air.

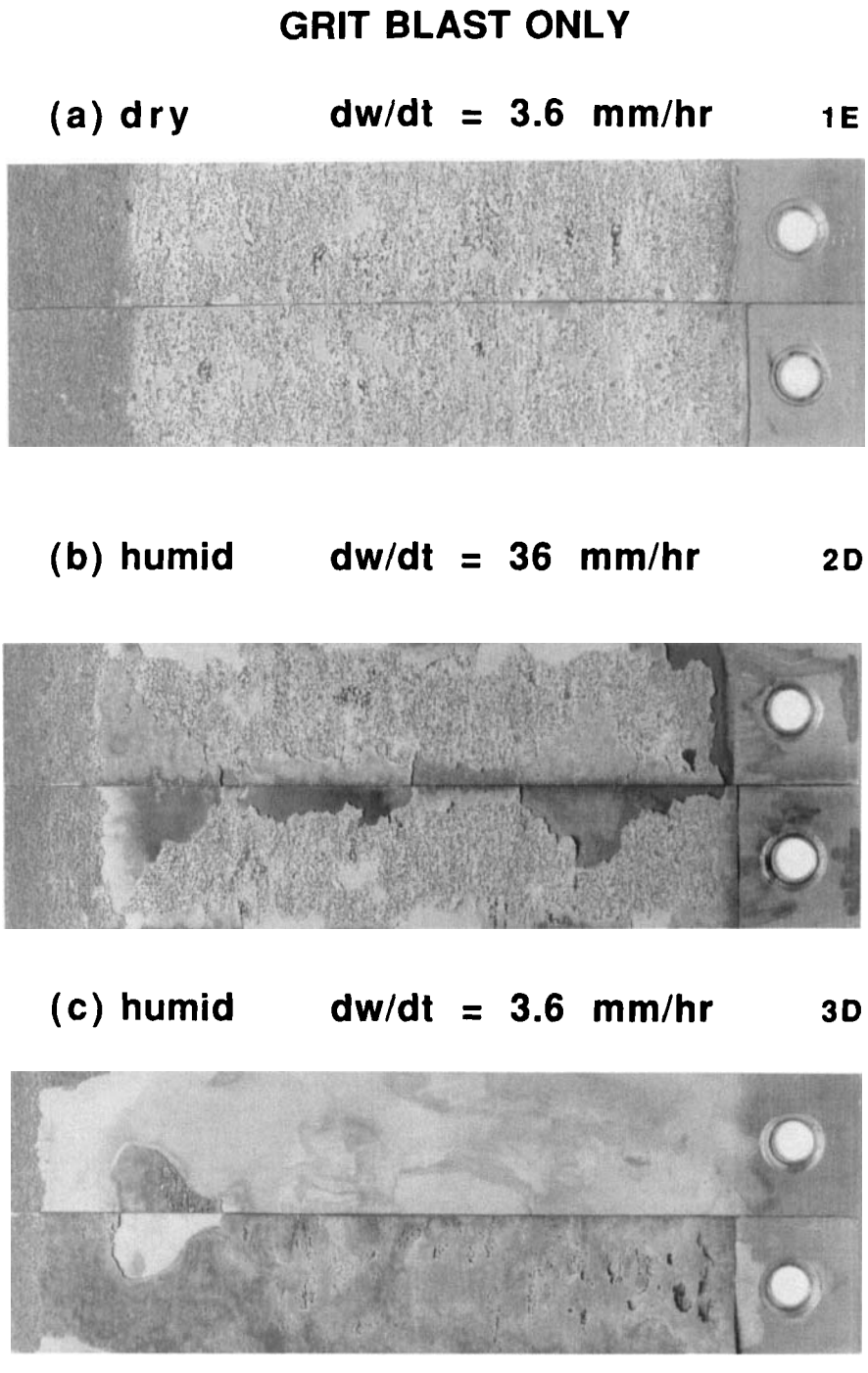

FIGURE 9 Photographs of fracture surfaces for three grit-blasted adherends. (a) warm dry air, $dw/dt = 3.6$ mm/hr. (b) warm humid air, $dw/dt = 36$ mm/hr. (c) warm humid air, $dw/dt = 3.6$ mm/hr.

Crack velocity is considered more relevant to the analysis of events occuring at the crack tip than load-point displacement rate. The crack velocity changes by a factor of 3 during a given test, but this is considered small in the context of the range of 10^3 in crack velocities used over the total number of tests. As the crack velocity is not constant for any test (equation (3)), data pairs of G_1 and crack velocity need to be calculated. In these tests, G_1 was calculated using equation (2) with data where w varied linearly with P^{-2}. The mean crack velocity was calculated by the "compliance" method using equation (4), where P was the mean of the load value set used to determine G_1. Crack velocity could be calculated directly from crack lengths measured with time, but this tends to introduce a bias toward the consideration of cracking at the specimen edges and does not avoid the need to choose a representative value of the data set. Figure 10 was replotted from the data used to plot Figure 8 curve (ii). In Figure 10(a), G_1 was plotted on a logarithmic scale to highlight the maximum and minimum values, *i.e.* $G_{max} = 1750\,Jm^{-2}$ and $G_{min} = 70\,Jm^{-2}$. In Figure 10(b), G_1 was plotted on a linear scale and in the shaded region (iii) shows the range of data where G_1 was unstable with crack velocity. The transitional crack velocity, v_{trans} representing data in the shaded region, was ≈ 5 mm/hr.

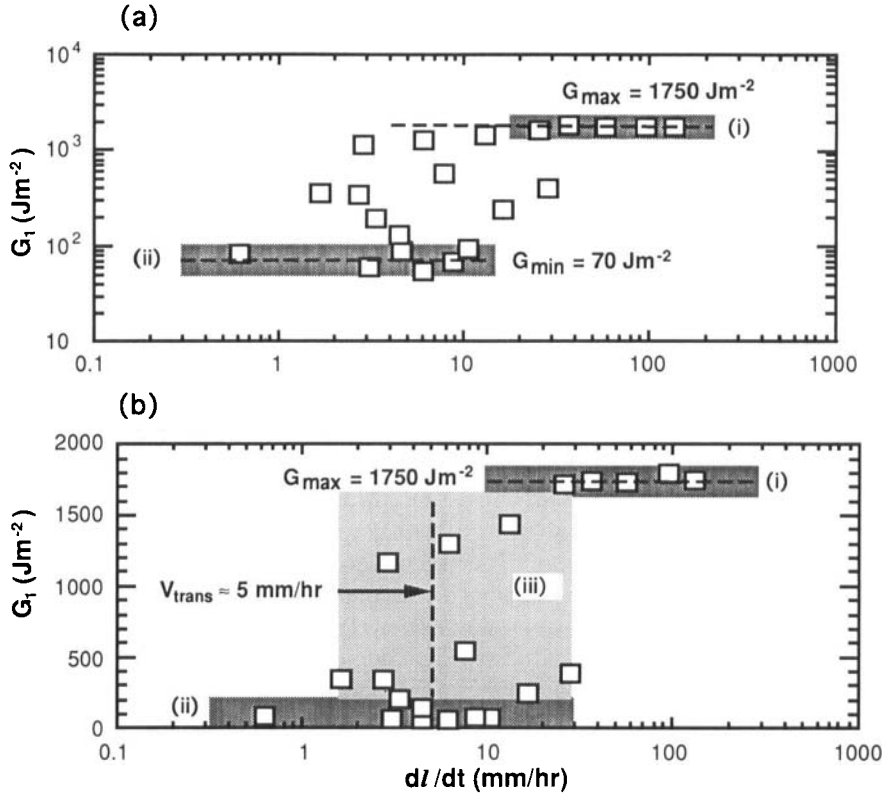

FIGURE 10 G_1 *versus* dl/dt for tests in warm humid air. (a) G_1 plotted on a logarithmic scale (b) G_1 plotted on a linear scale.

4 DISCUSSION

4.1 The Constant Displacement Rate Test

The specimen configuration used in the constant-displacement rate test (CDRT) is similar to that used in the Boeing wedge test[1] (Figure 1). Crack propagation in both tests is driven by elastic energy in the adherends. The fundamental differences between these two tests arises from the mode of loading the specimen.

In the CDRT, energy is continously supplied to the adherends as they are opened at a constant rate at their loading points (Figure 1b). When the crack propagates into material with uniform fracture properties, G_1 can remain constant over several centimetres of crack length (Figure 5). This generally constant G_1 indicates that the elastic energy released by the adherends is just sufficient to sustain crack propagation. In this case G_1 closely approximates the critical fracture energy of the bond, G_{1c}.

The crack velocity, dl/dt, as expected from equation (3), was found to change with crack length at constant dw/dt when G_1 was constant (Figure 7). For a typical case, the crack velocity at a crack extension of 90 millimetre is one-third that at 30 millimetre. As described in the results, the mean crack velocity was calculated from equation (4) with the mean of the load data set used to determine G_1. For most tests, the error in crack velocity will be at most $\pm 0.15\, dl/dt$. For the plot of G_1 *versus* dl/dt, shown in Figure 10, this error in crack velocity is small compared with the total range in dl/dt of 10^3.

G_1 was determined by two methods, both of which were based on equation (2). Zero load was coincident with the start of the test, whereas the zero of load-point displacement was arbitrary and was set when the load just commenced to rise (Figure 3). In one method, G_1 was determined from the gradient of a plot of w *versus* P^{-2} (Figure 5) where the chosen zero of load-point displacement has no influence on G_1. The intercept w', shown in Figure 5 as 0.7 mm, occurs at an apparent "infinite load" and is equivalent to the effective load-point displacement at crack initiation. This method for determining G_1 is preferred. The other method determines instantaneous values of G_1 by direct substitution in equation (2). Here, the zero of w must be corrected to coincide with crack initiation. Figure 6 shows that the instantaneous values of G_1 overshoot the mean value for initial correcting values w^* less than w' (≈ 0.7 mm in Figure 5) due to falsely high values of w in the calculations. Conversely, a choice of w^* greater than w' leads to undershoot. The plots of instantaneous G_1 in Figure 6 resemble damped oscillatory behaviour. This suggests that the bonded double-cantilever beam could be modelled by a second order feed-back control system.

Equations (1), (2), (3) and (4) were all derived without either a correction for the shear contribution to adherend elastic energy or a correction to the crack length for adherend rotation.[9,10] The shear contribution was considered negligible for crack lengths greater than 25 mm.[9] However, Stone and Peet[9] have demonstrated, with the Boeing wedge test, that ignoring an empirical correction to the crack length for adherend rotation can result in a 35% overestimate of G_1 at a crack length of 25 mm. This correction to crack length for adherend rotation can manifest itself through w in the CDRT. Correction to w is vital in estimating instantaneous G_1 as is shown in Figure 6. However, the preferred method for determining G_1 uses the gradient of a plot of w *versus* P^{-2}, where the absolute value of w is irrelevant.

In dry air tests, represented by Figure 8, curve (i), the fracture is principally cohesive (Figure 9(a)). Here, G_1 is relatively insensitive to changes in dw/dt, particularly at the lower values of dw/dt. To a first approximation, G_1 can be considered constant at low crack growth rates and it closely approaches G_{1c}. The slow decrease in G_1 as dw/dt decreases (Figure 8, curve (i)) could be explained in terms of the visco-elastic properties of the adhesive.

In humid air tests, water vapour diffuses into the specimen from both its edge and the crack front. Figure 8 curves (i) and (ii) show that G_1 is insensitive to humidity at high load-point displacement rates (or crack velocities) and approximates G_{1c} for an undegraded bond (Figure 8). However, the fracture surface of a specimen tested at a dw/dt of 36 mm/hr shows significant "adhesive" failure (Figure 9(b)) indicating that "adhesive" failure does not necessarily imply greatly reduced fracture toughness. At very low crack velocities, humidity has fully degraded the bond. Thus, the lower plateau $G_{\min}$ represents the fracture energy, G_{1scc}, for a degraded bond. The fracture in this case is "adhesive" (Figure 9(c)) and the G_{1scc} of approximately 70 Jm^{-2} shown in Figure 10 (a) is the fracture toughness of a fully-degraded bond. It is of interest to note that the shape of Figure 8 curve (ii) shows some similarity to the curves relating crack velocity to stress intensity factor for stress corrosion cracking in alloys.[12]

Figure 10 reveals a range in crack velocity where G_1 varies between $G_{\max}$ and $G_{\min}$. This transition in G_1 reflects a change in the severity of bond degradation. In order to interpret this transition, the moisture diffusion path must be understood. Moisture diffusion in the unstressed adhesive does not appear to cause bond degradation. This is because fracture surfaces created at the conclusion of tests by forced separation of the adherends appeared similar to failures in dry air (Figure 9(b)). Thus, bond degradation appears to be localised at the cracking zone where moisture may diffuse into the stressed adhesive both in the direction of crack propagation and from the specimen edges. The stained region near one edge on a fracture surface of the specimen shown in Figure 9(b) is attributed to degradation by liquid water. This water may either have diffused from the specimen edges or accumulated in the crack. The latter explanation is more likely as the feature shown in Figure 9 (b) is asymmetric and not typical of other specimens in the series. Ignoring this feature, the fracture surface shown in Figure 9(b), and on other specimens examined, did not show an increase in the fraction of "adhesive" failure as the test progressed. The absence of a progressive increase of "adhesive" failure with crack length further indicates that diffusion of moisture into the unstressed adhesive from the specimen edges is negligible. The transition range in G_1 is a consequence of the rates of crack advance and bond degradation being similar.

The decade range in crack velocity where the transition in G_1 occured, indicates that significant changes in bond durability can occur for each specimen having the same nominal adherend surface treatment. This variability can be explained in terms of:

(i) Changes in moisture concentration at the crack front for different tests and/or
(ii) Minor variations in surface treatment for different specimens.

In the case of moisture concentration, Figure 9(b) shows that condensed water causes more severe degradation than water vapour. In the case of minor variations in surface

treatment, previous work has shown that these can affect the crack velocity where the transition in G_1 occurred.[2] Both effects are expected.

Some tests conducted in humid air where the crack velocity was in the range corresponding to the transition in G_1 resulted in two linear segments in the *w versus* P^{-2} plot. In the first segment, G_1 tended toward G_{1c} whereas in the later segment, G_1 tended toward G_{1scc}. The existence of a linear segment suggests crack stability which is in accord with the Gurney and Hunt predictions for isotropic material and monotonically increasing displacement.[11] The comparatively abrupt change which occurred between the two linear segments suggests that crack propagation had undergone a transition, from a regime where the crack velocity was higher than the bond degradation rate to a regime where the crack velocity had fallen below the bond degradation rate.

The transitional crack velocity, v_{trans}, shown in Figure 10(b), represents the range of crack velocity where the transition in G_1 occurred and could be used as a bond durability indicator. This v_{trans} is a time-dependent quantity and describes a crack velocity which is similar to the rate of moisture diffusion ahead of the crack tip into a severely stressed adhesive bond. The CDRT is an accelerated test because the state of stress in the bond is more severe than that which would occur under service conditions. In the case of the grit-blasted adherends shown, v_{trans} is approximately 5 mm/hr, but the variation suggests that local crack velocities may vary considerably from this value. Thus, there are clear limitations to the precision obtainable with the CDRT in determining relative bond durabilities.

4.2 Comparisons with the Boeing Wedge Test

The Boeing wedge test[1] has proved to be reliable, qualitative method for comparing the durabilities of adhesive bonds in various environments and it correlates with service performance.[1,3] However, crack growth is a transient response to a single initial load point displacement. This has the consequence that fracture mechanics analyses lead to G_1 decreasing as the test progresses. The stress intensity in the cracking zone decreases as the adherend elastic energy decays and the crack decelerates. In dry tests, G_1 asymptotes to G_{1c} as the crack velocity tends to zero.

Boeing wedge tests are normally conducted in humid air on initially dry, pre-cracked specimens where crack growth had effectively ceased. On exposure to humid air, moisture diffuses into the stressed adhesive and degrades material ahead of the crack tip. Crack growth is resumed and G_1 decreases according to equation (1). As the crack extends, it decelerates and elastic energy stored in the adherends is dissipated. G_1 asymptotes toward G_{1scc} as the crack velocity tends to zero. Hardwick *et al.*[5] evaluated G_{1scc} after an arbitrary elapsed time of approximately 200 hours. Their G_{1scc} gives no indication of the possibility of further bond degradation which may lead to a shift in the zone of weakness in the bond structure. Baker[4] was concerned with bonds of more marginal durability than those of Hardwick *et al.*[5] His G_θ was evaluated after an arbitrary elapsed time 48 hours which exploited the crack velocity range where G_1 tended to be sensitive to adherend surface treatment.

Ideally, an evaluation of bond durability should be based on a time-dependent parameter. The equations describing G_1 are not time dependent and evaluations of

G_{1c} and G_{1scc} only require that sufficient time had elapsed to reach the steady state. None of the methods of fracture mechanics applied to the wedge test[4-9] lead to well-defined parameters describing the rate of bond degradation. By contrast, the CDRT reveals the range in crack velocity where crack propagation undergoes a transition from undegraded to degraded material. The transitional crack velocity, v_{trans}, or a similar indicator, is directly linked to the rate of bond degradation under apparent constant stress intensity at the crack tip. G_{1scc} is the fracture energy of a fully-degraded bond, is unambiguous and can be established with certainty provided that the lower plateau on plot of G_1 *versus* dl/dt is reached (Figure 10).

The ASTM Standard[1] for the Boeing wedge test specifies 3.2 mm thickness for aluminium alloy adherends. Adherend treatments, adhesives and test conditions leading to G_1 greater than 1900 Jm^{-2} will result in plastic bending of 3.2 mm thick adherends (equation (5)). For the Boeing wedge test, G_1 is initially much higher than G_{1c}. Conversely, for the CDRT, G_1 only just exceeds G_{1c} for dry tests. It is clear that for valid fracture mechanics calculations the adherend thickness is higher for the Boeing wedge test than for the CDRT. It is not surprising that for Boeing wedge tests, plastic bending often occurs in the adherends for tough adhesives.

4.3 Practical Relevance of the Constant Displacement-rate Method.

The constant displacement-rate method is a powerful instrument to develop further scientific insight into adhesive bonding mechanisms, since the crack velocity can be manipulated by varying the load-point displacement rate. The CDRT measures G_1 at near-equilibrium conditions and leads to a crack velocity directly relevant to bond durability. It can evaluate the fracture energy for both undegraded and degraded bonds. As a practical method for ranking bond durability, the Boeing wedge test is much faster than the CDRT as it can interrogate a wide range of crack velocities in one test.[5] The authors intend to develop the CDRT to measure G_1 at several discrete load-point displacement rates, also in one test. Marceau *et al.*[1,3] have reported that the Boeing wedge test reflects the relative durability of bonds in service and, thus, it is reasonable to expect that the CDRT will also reflect service durability.

5 CONCLUSIONS

1. The CDRT is a quantitative procedure where G_1 is determined from two accurately measured quantities; *viz.* load and load-point displacement. Under conditions where a crack is propagating into uniform material, G_1 was found to be essentially constant.
2. The CDRT leads directly to a G_{1c} value for an undegraded adhesive bond and a value of G_{1scc} for a degraded bond.
3. The CDRT provides sufficient control over the crack velocity to measure the rate of environmental degradation of stressed adhesive bonds.
4. The CDRT reveals a range in crack velocity where crack propagation undergoes a transition from an undegraded to a degraded adhesive bond. This leads to a transitional crack velocity which may serve as bond durability indicator.

6 Acknowledgements

The authors gratefully acknowledge discussion with and contributions from Dr A. A. Baker and Dr R. J. Chester. The authors also acknowledge constructive comments from the referees of this paper.

7 References

1. "Standard Test Method for Adhesive-Bonded Surface Durability of Aluminium (Wedge Test)", ASTM-D3762-79 (ASTM, Philadelphia).
2. D. R. Arnott and M. R. Kindermann, Proceedings of The Australian Aeronautical Conference 1989, Melbourne, 9-11 Oct 1989, pp. 192–196.
3. J. A. Marceau and E. W. Thrall, "Environmental-Durability Testing", in *Adhesive Bonding of Aluminium Alloys*, E. W. Thrall and R. W. Shannon, Eds. (Marcel Dekker, N. Y., 1985), pp. 177–197.
4. A. A. Baker, *Composites* **18**, 293 (1987).
5. D. A. Hardwick, J. S. Ahearn and J. D. Venables, *J. Mater. Sci.* **19**, 223 (1984).
6. J. Cognard, *J. Adhesion* **20**, 1 (1986).
7. D. Broek, *Elementary Engineering Fracture Mechanics*, (Martinus Nijhoff 1986), p. 128.
8. C. Gurney and R. Amling, *in Adhesion Fundamentals and Practice*, (McLaren, 1969), pp. 211–217.
9. M. H. Stone and T. Peet, "Evaluation of the Wedge Test for Assessment of Durability of Adhesive Bonded Joints", Royal Aircraft Establishment Tech Memo, Mat 349, July 1980.
10. S. Mostovoy, P. B. Crosley and E. J. Ripling, *J. Materials* **2 (3)**, 661 (1967).
11. C. Gurney and J. Hunt, *Proc. Roy. Soc A* **299**, 508 (1967).
12. M. O. Spiedel, in *The Theory of Stress Corrosion Cracking in Alloys*, J. C. Scully, Ed. (NATO, Brussels, 1971), p. 300.

NOMENCLATURE

CDRT	constant displacement rate test.
G_1	elastic energy release rate (crack extension force).
G_{1c}	critical fracture energy for an undegraded bond.
G_{1scc}	critical fracture energy for a full-degraded bond.
P	load.
w	load-point displacement.
w'	load-point displacement at an apparent infinite load.
w^*	arbitrary initial correction to the load-point displacement.
w_c	w-w^*.
dw/dt	load-point displacement rate.
h	adherend thickness.
b	width of adherends.
E	Young's modulus of the adherends.
σ_y	yield stress of the adherends.
l	effective length of the cantilevered adherends.
dl/dt	crack velocity.
v_{trans}	transitional crack velocity representing the transition region in G_1.